Applied Surface Science 256 (2010) 3116–3121

Contents lists available at ScienceDirect

Applied Surface Science

journal homepage: www.elsevier.com/locate/apsusc

Enhanced photocatalytic activity of silver metallized TiO_2 particles in the degradation of an azo dye methyl orange: Characterization and activity at different pH values

L. Gomathi Devi *, K. Mohan Reddy

Department of Chemistry, Bangalore University, Central College City Campus, Dr.B.R. Ambedkar Veedhi, Bangalore 560001, Karnataka, India

ARTICLE INFO

Article history:
Received 31 October 2009
Received in revised form 26 November 2009
Accepted 26 November 2009
Available online 2 December 2009

Keywords:
Silver deposited titanium dioxide
Methyl orange
Photocatalytic degradation

ABSTRACT

The photocatalytic activity of silver deposited Degussa P25 titanium dioxide (Ag-DP25) in the photodegradation of methyl orange (MO) was investigated. The photocatalysts were characterized using PXRD, SEM, EDX, FTIR and UV–vis spectrophotometer. The obtained results show that the silver (Ag^0) deposited TiO_2 exhibited visible light plasmon absorption band. The degradation experiment reveals that the catalytic property of Ag-DP25 in the degradation of MO is more efficient than that of commercially available Degussa P25 TiO_2 (DP25) samples. The improvement of Ag-DP25 catalyst efficiency strongly depends on the content of silver (Ag) deposits. The present study shows that the degradation process is dominated by Ag–TiO_2 photocatalytic system, complying with pseudo-first order rate law. The higher rate of photodegradation observed on Ag-DP25 at pH 6.6 can be correlated to the ratios of the concentrations of the ionized to the neutral dye molecules and also to the higher concentration of hydroxylated surface, which are able to effectively scavenge photogenerated valence band holes. Accumulation of the holes in the semiconductor particles increases the probability of formation of excited oxygen atom which is a reactive species readily oxidizing the organic dye molecule. The reduction of pH during the course of the reaction is attributed to the complete mineralization of the dye.

1. Introduction

Photocatalysis on semiconductor TiO_2 has been widely investigated in recent years, mainly because of its high potential for ensuring the complete destruction of organic contaminants in the aqueous medium [1–5]. Titanium dioxide is the most extensively studied photocatalytic material, with outstanding physical and chemical properties. On excitation, electrons are promoted to the conduction band and holes are consequently generated in its valence band. Such charge carriers are able to reduce and oxidize many species adsorbed on the semiconductor particles and induces the oxidative destruction of organics upto their mineralization [6–11]. The high rate of recombination between photogenerated electron-hole pairs is a major rate-determining factor controlling the photocatalytic efficiency. In this regard, noble metal deposition can improve the photocatalytic efficiency of titanium dioxide [12–16], by trapping the electrons thereby preventing the recombination. Metal islands deposited on the semiconductor surface have been shown to efficiently trap the electron and the free hole in the valence band can successively participate in the oxidation reactions [17]. The equilibration of the Fermi-level between the metal and the semiconductor favors electron accumulation in the composite metal/TiO_2 system. Kim et al., reported that silver was more effective than platinum in the plasma-driven catalyst reactor packed with TiO_2. The deposition of Ag nanoparticles on the Degussa P25 titanium dioxide (DP25) surface is explained in the present study as a means of improving its photocatalytic activity in the degradation of MO in the aqueous phase under UV irradiation. The effect of pH on the photocatalytic activity of metallized semiconductor particles is explored.

Under UV-light irradiation, the photogenerated electrons quickly transfer from TiO_2 surface to the Ag particles, leading to the effective separation of electron-hole and results in the improvement of photocatalytic efficiency. The noble metals such as Pt [18,19], Ag, and Au [9,20] deposited TiO_2 have the high Schottky barriers among the metals and thus act as electron traps, facilitating electron-hole separation and promotes the interfacial electron transfer process [21,22]. However, the studies on nanocrystallites of silver deposited photocatalyst are still limited in the literature [23].

The aim of the present work is to prepare Ag deposited TiO_2 (Ag-DP25) by a photodeposition method on Degussa P25 (DP25) and to

* Corresponding author. Tel.: +91 80 22961336; fax: +91 080 22961331.
E-mail address: gomatidevi_naik@yahooo.co.in (L. Gomathi Devi).

0169-4332/$ – see front matter © 2009 Elsevier B.V. All rights reserved.
doi:10.1016/j.apsusc.2009.11.083

compare the activity of the photocatalyst before and after the surface modification.

2. Experimental

2.1. Materials

Photocatalyst TiO_2 Degussa P25 (DP25) (reported surface area ~50 $m^2\ g^{-1}$) was used as a starting material to prepare Ag-DP25. Silver nitrate ($AgNO_3$), sodium hydroxide (NaOH) and sulphuric acid (H_2SO_4) were obtained from Merck chemicals, methyl orange (MO) (dimethyl amino-azobenzene sodium sulphonate) is obtained form Aldrich chemicals whose molecular formula is $(CH_3)_2NC_6H_4NNC_6H_4SO_3Na$ and the formula weight is 327 and shows a λ_{max} of 460–480 nm. All the reagents used were of analytical grade and the solutions were prepared using double distilled water.

2.2. Preparation of silver deposited TiO_2 powders

Ag-DP25 photocatalyst is prepared based on the reduction of $AgNO_3$ in the presence of oxalic acid in DP25 suspension as prepared by Szabo-Bardos et al. [12]. Metallic silver is deposited on DP25 (Ag-DP25) surface by photodeposition method. An aqueous solution of $AgNO_3$ (2×10^{-4} M), oxalic acid (5×10^{-3} M) along with DP25 (1 g) were added to 1 L of distilled water stirred vigorously. The pH of the suspension was adjusted to 6.8–7.0 by the addition of 0.1N NaOH solution and the suspension is irradiated with UV-light for 40–50 min, after the irradiation the solution containing Ag–TiO_2 was then allowed to stand for 6 h. The colour of the reaction mixture was observed to be changed from white to violet-brown under UV-light indicating the reduction of Ag^+ to Ag^0 and deposition of Ag^0 on DP25. The brown solid is filtered, dried and was heated at 120 °C for 2 h in an incubation to evaporate water and the colour of the solid catalyst changes to pale pink which confirms the deposition. The absence of silver in the aliquot sample of reaction mixture confirms the deposition of noble metal on the semiconductor particles.

2.3. Analytical techniques

The PXRD patterns were recorded using Bruker aXS Model D8 Advanced powder X-ray diffractometer with a Cu Kα source (λ = 1.541 A°) and the scanning range employed was 2θ = 5–85° at a scan rate of 2° per minute. The average crystallite size was calculated using the Scherrer's formula. The X-ray diffraction line broadening was obtained with a slow scanning speed of 1/2° per minute. The particle size is obtained by SEM analysis of the samples using JEOL-JSM-6490LV scanning electron microscopy. The EDX analysis was done using Oxdord INCA 250 energy dispersive X-ray microanalyzer. The absorption and diffuse reflectance spectra were recorded by using double beam UV-3101PC UV–vis-NIR Shimadzu scanning spectrophotometer. The spectra were recorded at room temperature in the range of 200–800 nm. FTIR spectra were recorded using FTIR-840OS SHIMADZU FTIR spectrophotometer, in the range of frequencies from 4000 to 400 cm^{-1} using KBr as the reference sample.

2.4. Photocatalysis procedure

The degradation experiments were carried out in the 1000 mL reactor equipped with medium pressure mercury vapour lamp with a photon flux of 7.75 mW/cm^2 (as determined by ferrioxalate actinometry) whose wavelength is around 350–400 nm is used. The reaction mixture was magnetically stirred during the course of reaction at ambient temperature. 250 mL of aqueous dye solution (10 ppm) along with 40 mg of the photocatalyst (DP25/Ag-DP25) is irradiated with UV-light. The initial pH of the MO aqueous suspension was found to be 6.6. 3 mL of sample was periodically withdrawn from the reactor and analysed after removal of DP25 particles by centrifugation at 3000 rpm for 15 min. The cleavage of the azo bond of MO leading to its bleaching was monitored by spectrophotometric analysis at 475 nm.

3. Results and discussion

3.1. Characterization of photocatalysts DP25 and Ag-DP25

The absorption and diffused reflectance UV–vis spectra of DP25 and Ag-DP25 are shown in Figs. 1 and 2. The strong plasmon resonance absorption at wavelengths above 400 nm is observed due to the Ag nanoparaticle deposition on DP25. Light absorption by the deposited metal causes a collective oscillation of the free conduction band electrons of the silver nanoparticles as a consequence of their optical excitation. This phenomenon is observed when the wavelength of the incident light far exceeds the particle diameter.

Hermann and Sclafani [18] have proposed a mechanism describing the deposition and growth of silver particles on the titania surface. Silver ions are initially adsorbed on the surface of TiO_2 particles. Photogenerated electrons reduce adsorbed Ag^+ ions to silver metal atoms. The formation of small crystallites of silver can occur either by the agglomeration of silver atoms or by a cathodic-like successive reduction process. The agglomeration of silver atoms can be described in the following way

$$TiO_2(e^-, h^+) + Ag^+\text{adsorbed} \rightarrow TiO_2Ag^0(h^+) \quad (1)$$

The successive reduction sequence is represented by

$$mAg^0 \rightarrow Ag_m \quad (2)$$

In UV–vis absorption/diffuse reflectance spectroscopy, DP25 particles exhibit strong absorption band at ~400 nm [24], which corresponds to the band gap energy of 3.0–3.2 eV. Pure colloidal silver exhibits an absorption band at ~500 nm which is normally attributed to the typical surface plasmon absorption of silver nanoparticles. The Ag-DP25 semiconductor particles exhibited an extended absorption in the range of 500–800 nm (Figs. 1 and 2) in addition to the typical DP25 absorption profile. The reason for such a broad absorption band may be attributed to the plasmon effect shown by the silver nanoparticles.

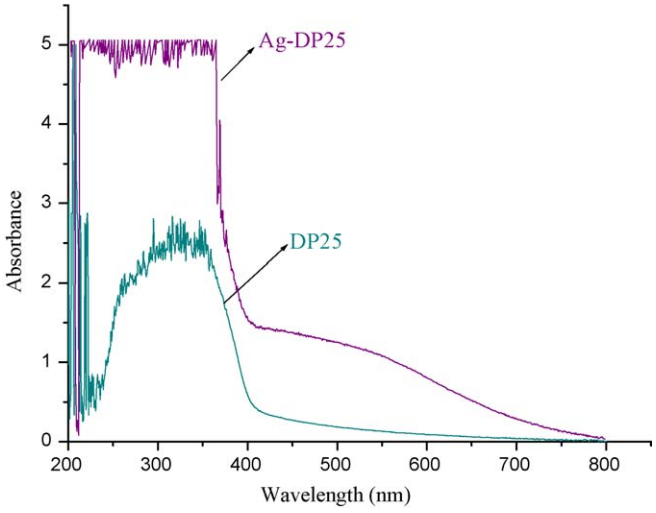

Fig. 1. Plot of UV–vis absorbance spectra for Ag-DP25 and DP25 photocatalysts.

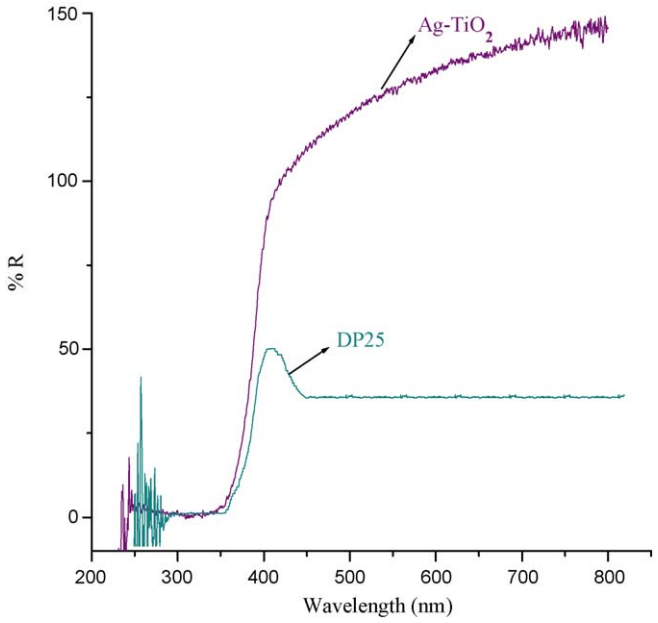

Fig. 2. Plot of % reflectance versus wavelength for Ag-DP25 and DP25 photocatalysts.

Fig. 3 shows the powdered X-ray diffraction (PXRD) patterns of pure DP25 and Ag-DP25 catalysts. The PXRD pattern shown in the figure consisted of mainly anatase with minor rutile phase (80:20) [25]. The 2θ values at which major peaks appear for Ag-DP25 are found to be almost the same as that of pure DP25. This may be due to the fact that deposition does not alter the crystal structure of Ag-DP25. Diffractions that are attributable to anatase (A)/rutile (R) phase of DP25 crystals are clearly detectable at 2θ values of 25.285° (A) (3.51943)/27.439° (R) (3.24795) (the numbers in the parenthesis represents the d-spacing values for A and R, respectively). Slow scanning (1/2°/min) shows a peak at $2\theta = 37.874°$ (Ag) (2.37360) in Ag-DP25, which can be assigned to (2 0 0) plane of silver which confirms the deposition of Ag on the surface of DP25. The anatase/rutile lattice structure of pure DP25 is unperturbed in the PXRD pattern of Ag-DP25. Silver deposition did not affect the phase structure of DP25 as the Ag phase being hardly detectable in 0.23% Ag deposited on Ag-DP25.

In order to investigate the morphology of the synthesized photocatalyst particles SEM analysis and energy dispersive X-ray microstudies were performed. Fig. 4a–d shows SEM images of the DP25 and Ag-DP25 particles at two different magnifications. The images illustrate that the particles are spherical and have a smooth surface in Ag-DP25 due to the deposition of silver. This photodeposition method leads to heterocoagulation where the nanosized Ag deposits are formed on the surface of DP25 spheres. Qualitative determination of Ag-DP25 was studied by EDX technique as shown in Fig. 5 by using grid supported carbon film of 15–25 nm thickness which gives exceptionally low background. The atomic % and weight % values are represented in Table 1.

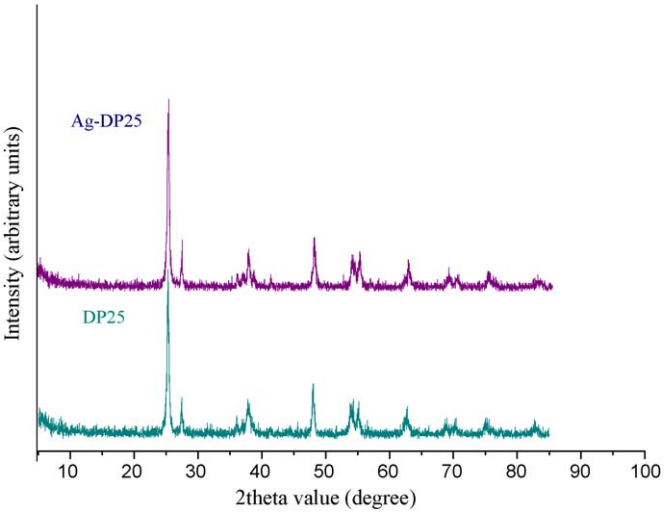

Fig. 3. The PXRD pattern of Ag-DP25 and DP25 photocatalysts.

The infrared spectra of DP25 and Ag-DP25 powders in the range 4000–400 cm^{-1} shows a broad band at 3400 cm^{-1} which can be assigned to γ_{OH} stretching mode of O–H vibration of the Ti–OH. The other narrow band at 1640 cm^{-1} can be assigned either to δ_{OH} bending modes of hydroxyl group or to the stretching mode of Ti–O (γ_{Ti-O}) which could be the envelope of the bands of Ti–O–Ti bond of a titanium oxide network. This band increases in its intensity for Ag-DP25 suggesting the surface to be more hydroxylated compared to DP25.

3.2. Photocatalytic activity

Preliminary tests, performed to verify the adsorption properties of photocatalysts show that the adsorption was high on Ag-DP25. The extent of adsorption of MO was determined, after continuous stirring for one hour in the dark at laboratory temperature using the formula $Q = ((C_0 - C_e)V)/W$, where Q is the extent of adsorption, C_0 and C_e are concentrations before and after adsorption at equilibrium, V is the volume of the reaction mixture and W is amount of catalyst added. The value of Q is found to be 5.123×10^{-3} ppm mL mg^{-1}. The isoelectric point of Ag-DP25 has been reported to shift to lower pH values with respect to unmodified DP25, thus, extending the pH region where the photocatalyst surface is negatively charged. This inhibits the adsorption of negatively charged dye radicals such as the bisulphonic azo dye MO. The first order kinetic rate constant for the photocatalytic degradation of MO is reported in Table 2. Fig. 6 gives the MO photomineralisation profile with DP25 and Ag-DP25 suspensions and is monitored by UV–vis spectral analysis.

3.3. Effect of pH

The effect of pH on the rate of MO photodegradation was investigated in the presence of DP25 and Ag-DP25. The results obtained in the pH range 3–9 are given in Table 3 which shows that the enhanced photodegradation was obtained at pH 6.6 for both the catalysts. MO is red coloured below pH 3 and appears yellow above 4.5 ($pK_{in} \approx 3.7$) and the colour depends upon the concentration of H^+ and OH^- ions. The concentration of the ionized indicator [MO^-] and protonated indicator [HMO] in acidic solutions, and the concentration of hydroxylated indicator [MOOH] and ionized indicator molecule [MO^+] in alkaline solutions determine the adsorption characteristics. In the presence of excess [H^+] ions in the solution, the ionization will be depressed due to the common ion effect and the concentration [MO^-] will be very small and the colour will therefore be that of unionized form. In the alkaline medium the decrease of [H^+] will result in the further ionization of the indicator thereby increasing the colour of the ionized form. The concentration of the ionized and unionized forms is thus directly related to the hydrogen ion concentration. The ratios of [MO^-]/[HMO] and [MOOH]/[MO^+] in acidic and basic solutions determines the adsorption characteristics on the surface of photocatalysts. The point of zero charge (pzc) of the photocatalyst also varies with pH. Below the isoelectric point the surface

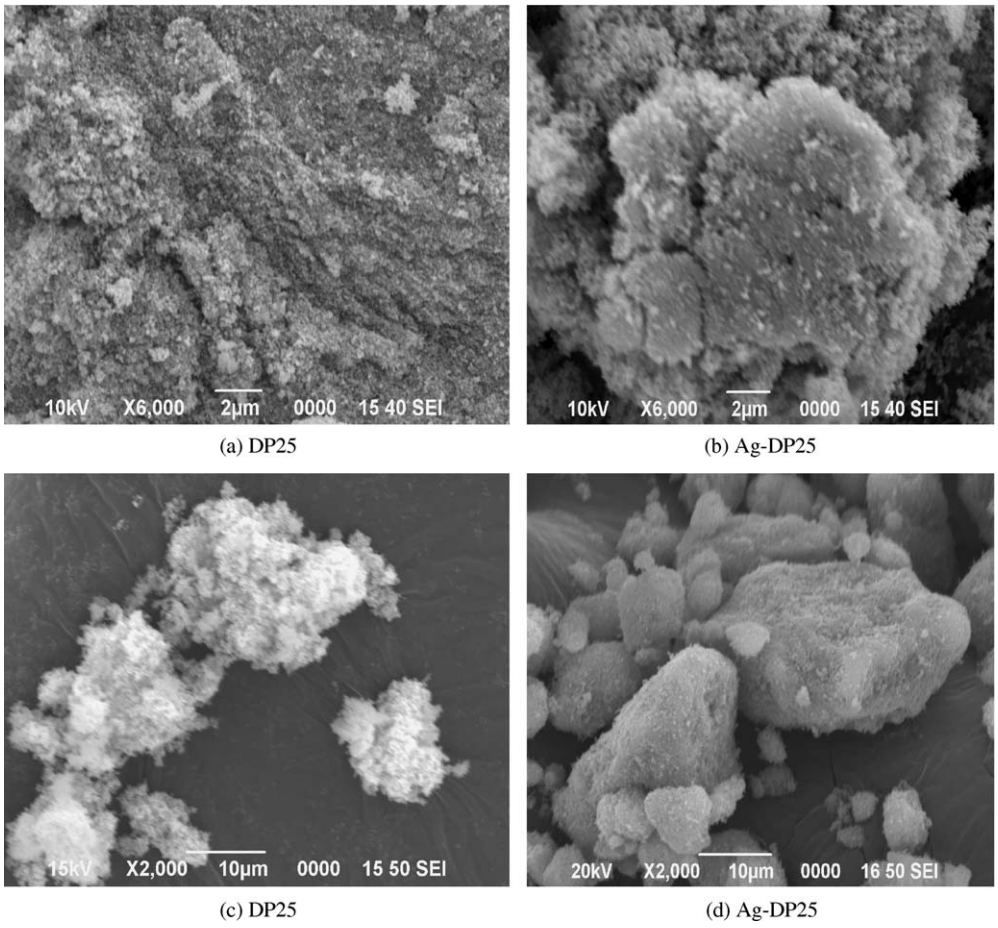

Fig. 4. (a–d) SEM images of Ag-DP25 and DP25 photocatalysts at two different magnifications.

is positively charged and vice versa. The combined effect of surface charges and ionized concentration of dye molecules will determine the extent of adsorption. Maximum adsorption was observed at pH 6.6 for both the photocatalysts. But the extent of degradation was higher with Ag-DP25 in the specified time interval. Due to the multiple roles that various factors could play, such as electrostatic interactions with the semiconductor surface, chemical structure of the target molecule and of its fragments or intermediate formation of active radicals, etc., will dictate the reaction process. Further the capacity of adsorption on DP25 and Ag-DP25 at different pH values can be explained by the intrinsic amphoteric behaviour (Ti–OH) of suspended catalyst particles and the acidic/basic nature of the dye molecule. The metal oxide photocatalyst particles in aqueous system behave as diprotic acids due to the surface hydroxylation. This photocatalyst surface have active role in the photodegradation reaction.

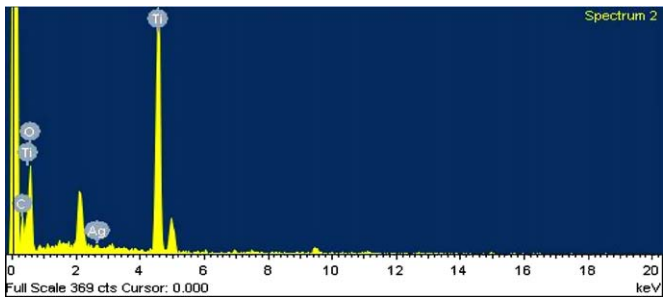

Fig. 5. EDX spectra of 0.23 at.% Ag-DP25 photocatalyst.

In acidic solution, the possible reactions are:

$$TiOH + H^+ \rightarrow TiOH_2^+ \qquad pH < 6.25 \tag{3}$$

$$TiOH \rightarrow TiO^- + H^+ \qquad pH > 6.25 \tag{4}$$

Due to the higher extent of hydroxylation on Ag-DP25 (as supported by the FTIR spectroscopic studies) the extent of adsorption of reactive dye molecules seems to be higher [13]. The higher efficiency of metalized Ag-DP25 can be attributed to (i) high electron affinity by deposited metal and hence increase of lifetime of charge carriers thereby decreasing the rate of recombination, (ii) increase in the absorbed light fraction due to the shift in the absorption spectrum of semiconductor to the longer wavelength (iii) accumulation of the holes in the semiconductor particles increases the probability of formation of excited oxygen atom which are reactive species and readily oxidizes the organic dye molecule.

The various possible reactions at Ag-DP25 surface is as follows

$$e^-(\text{trapped at Ag deposit}) + O_2 \rightarrow O_2^{\bullet -} \tag{6}$$

$$O_2^{\bullet -} + H^+ \rightarrow HO_2^{\bullet} \tag{7}$$

Table 1
The results of EDX analysis of Ag deposited DP25 sample.

Element	Weight %	Atom %
Oxygen (O)	10	77
Titanium (Ti)	7	23
Silver (Ag)	0.1	0.2

Table 2
Pseudo-first order rate constants and the corresponding regression coefficient for the photodegradation of MO.

Photocatalyst	k (min^{-1})	R^2
Ag-DP25	7.765×10^{-2}	0.9874
DP25	4.521×10^{-2}	0.9458

The excess electrons at the Ag deposits can further modify $O_2^{\bullet-}$

$$e^-(\text{trapped at Ag deposit}) + O_2^{\bullet-} \rightarrow O_2^{2-} \quad (8)$$

This adsorbed peroxide ion can dissociate to O^-, and this further reacts with hole producing an excited oxygen atom [21,26]

$$O_2^{2-} \rightarrow 2O^- \text{ (absorbed)} \quad (9)$$

$$O^- + h^+ \rightarrow O* \quad (10)$$

The decrease of pH in the course of the degradation reaction can be accounted to the continuous decomposition of MO and the formation of simple ions like NO_3^-, SO_4^{2-}, CO_2 and H_2O. Effects of pH on the degradation of MO dye indicated that the photocatalytic degradation of MO over Ag-DP25 was significantly affected by the solution pH. The degradation rate of MO decreased drastically with increase or decrease of pH. 100% and 76% of the removal rate of MO were accomplished at pH, 6.6 using Ag-DP25 and DP25, respectively, after 60 min of UV irradiation. However, only 43% and 51% of MO was degraded at pH 3.0 and 9.0, respectively using Ag-DP25. When pH was higher than 6.6, the surface potential of Ag–TiO_2 particle was negative. In an aqueous medium, MO molecule ionizes as MO anion and two sodium cations. The electrostatic repulsion between MO anion and photocatalyst particle increased and the adsorbed amount of MO decreased with increase of pH, resulting in decrease in degradation rate for MO. Further the positions of both valence and conduction band depend on the pH of the solution and the potential of these bands shifts by 59 mV more towards the negative potential as the pH increases by one unit at 25 °C [27].

3.4. UV–vis spectral analysis for the photocatalytic degradation of MO

Photochemical breakdown of the chromophoric groups (–N=N–) present in the MO molecule is monitored by UV–vis spectrophotometer. The colour of the samples decreased progressively to about 40% in 15 min, and almost 99% within 60 min

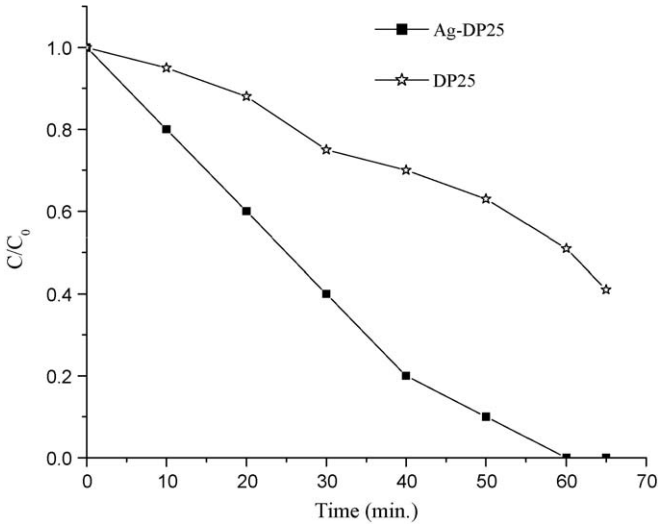

Fig. 6. Plot of C/C_0 versus time (min) for MO photodegradation using DP25 and Ag-DP25photocatalysts.

Table 3
Effect of pH and the % of degradation of MO using DP25 and Ag-DP25 photocatalyst for the illumination of a time period of 60 min.

Photocatalyst	pH	% degradation
Ag-DP25	3.0	43
	5.0	72
	6.6	100
	9.0	51
DP25	3.0	31
	5.0	51
	6.6	76
	9.0	39

duration. The observed strong absorbance at wavelength lower than 250 nm, imply the fragmentation of the MO molecule leading to the formation of transient species whose degradation requires a longer reaction time. MO is characterized by a band in the range 480–465 nm in the visible region attributed to azo form and the bands at 280 and 198 nm are due to the presence of the benzene rings. Under progressive protonation colour of the solution changes from orange yellow to red due to the formation of mono protonated form of MO, which exists as resonance hybrid between its quine diamine and azonium structures. The visible region band can be attributed to azonium ions. On irradiation along with catalyst, band at 475 nm completely disappears at 15 min. Only band at 200 nm retains up to 40 min of irradiation. This band can be attributed to benzene. At 70 min of irradiation, this band completely diminishes indicating complete degradation of the dye.

3.5. Determination of COD

The chemical oxygen demand (COD) was determined by using standard dichromate method, based on the formula

$$\text{COD}\,(O_2\ \text{mg/L}) = \frac{V_0 - V_1 \times N \times 8 \times 1000}{V_2},$$

where N is the concentration and V_1 is the volume of $(NH_4)_2Fe(SO_4)_2$ titrant, V_0 is the volume of $(NH_4)_2Fe(SO_4)_2$ titrant used in the blank and V_2 is the volume of water sample. Percentage COD removal efficiency using different dosages of Ag-PD25 and DP25 is shown in Fig. 7 degradation rate is strongly dependent on the dosage of Ag-DP25 added. The lower dosage of Ag-PD25 shows lower percentage of COD removal, while optimal dosage 40 mg of Ag-DP25 increases the percentage of COD removal efficiencies. Test samples were collected at every 15 min time interval and COD was measured using dichromate titrimetric method. The calculated COD values decrease continuously during the process of degradation. Finally, the percentage of COD removal is calculated using the formula

$$\text{percentage of COD removal} = \left[\frac{(\text{COD}_{\text{blank sample}} - \text{COD}_{\text{MO samples}})}{\text{COD}_{\text{blank sample}}}\right] \times 100$$

3.6. Reaction kinetics

Photocatalytic degradation of MO fit well with the pseudo-first order equation and was confirmed for both the Ag-DP25 and DP25 catalysts.

$\ln(C_0/C) = k(t)$, where C_0 is the initial concentration (ppm) of the dye; C is the concentration (ppm) of the dye at time t; t is the irradiation time (min); k is the reaction rate constant (min^{-1}); the apparent rate constants for the above catalytic process is found to be 7.765×10^{-2} min^{-1}, R^2 is 0.9874 and 4.521×10^{-2} min^{-1}, R^2 is 0.9458, respectively.

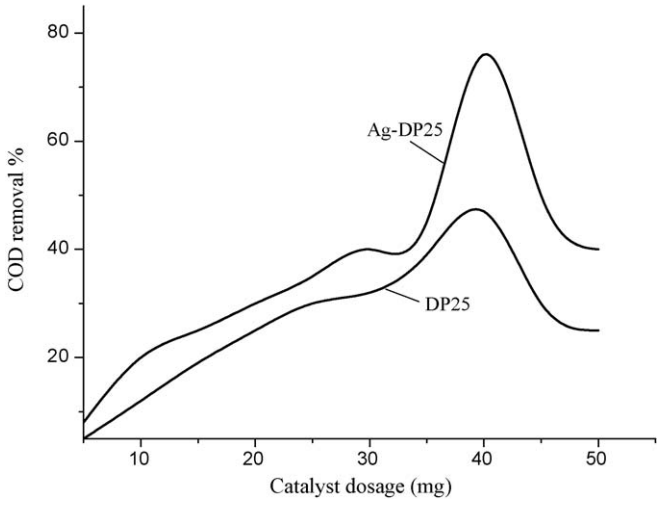

Fig. 7. Percentage of COD removal of MO using Ag-DP25 and DP25 catalysts at different dosages.

4. Conclusion

The deposition of nanosized silver particles on the DP25 surface increases the photocatalytic activity of the semiconductor oxide, by increasing the efficiency of charge separation of the photo-generated electron-hole pairs. The presence of silver mainly enhances the photocatalytic oxidation of organic compounds that are predominately oxidized by holes. Though crystal structure, specific surface area, particle size and size distribution is same for both the catalysts the enhancement in the degradation was observed for Ag-DP25. The enhancement is due to the electron trapping by the metal deposit, higher extent of light absorption and degree of hydroxylated surface will dictate the photocatalytic reaction in Ag deposited catalyst. Further, accumulation of the holes in the semiconductor particles increases the probability of formation of excited oxygen atom which is a reactive species and readily oxidizes the MO dye molecule. The degradation is most efficient at pH 6.6 for both the catalysts which depends on the concentration of the various ions formed and also on the nature of the catalyst. But the extent of degradation was higher with Ag-DP25 in the specified time interval. This is due to the higher extent of surface hydroxylation on Ag-DP25 leading to the higher extent of adsorption of reactive dye molecules. The combined effect of surface charges and ionized concentration of dye molecules will determine the extent of adsorption. It was found that under optimal experimental conditions the percentage of COD removal is found to be 76% at pH 6.6.

Acknowledgements

Financial assistance from Department of Science and Technology (DST) Major Research Project (2009–2012), Government of India is greatly acknowledged.

References

[1] M. Schiavello (Ed.), Photocatalysis and Environment. Trends and Applications, Kluwer Academic Publishers, Dordrecht, 1988.
[2] E. Pelizzetti, N. Serpone (Eds.), Photocatalysis. Fundamentals and Applications, Wiley, New York, 1989.
[3] M.R. Hoffmann, S.C. Martin, W. Choi, D.W. Behnemann, Chem. Rev. 95 (1995) 69–96.
[4] A. Hogfelt, M. Gretzel, Chem. Rev. 95 (1995) 49–68.
[5] J.M. Herrman, H. Tahiri, Y. Ait-Ichou, G. Lassaletta, A.R. Gonzalaz-Elipe, A. Fernandez, Appl. Catal. B: Environ. 13 (1997) 219–228.
[6] M.A. Fox, M.T. Dulay, Chem. Rev. 93 (1993) 341–357.
[7] A. Heller, Acc. Chem. Rev. 28 (1995) 503–508.
[8] M. Anpo, H. Yamashita, in: M. Anpo (Ed.), Surface Photochemistry, Wiley, Chichester, 1996, pp. 117–164.
[9] P.V. Kamat, Chem. Rev. 93 (1993) 267–300.
[10] D.M. Blake, P.C. Maness, Z. Huang, E.J. Wolfrum, J. Huang, W.A. Jacoby, Sep. Purif. Methods 28 (1999) 1–50.
[11] A. Agostiano, A. Albini, F. Bordin, J.P. Fouassier, M.P. Gordon, H. Lemmetyinen, U.E. Steiner, T. Yagishita, Trends Photochem. Photobiol. 4 (1997) 79–86.
[12] E. Szabo-Bardos, H. Czili, A. Horvath, J. Photochem. Photobiol. A: Chem. 154 (2003) 195–201.
[13] E. Szabo-Bardos, H. Czili, A. Horvath, J. Photochem. Photobiol. A: Chem. 184 (2006) 221–227.
[14] W.D. Kingery, H.K. Bowen, D.R. Ulmann, Introduction to Ceramics, Wiley-Interscience, New York, NY, 1976, p. 457.
[15] A. Sarkany, Z. Revay, Appl. Catal. A: Gen. 243 (2003) 347–355.
[16] H.H. Kim, S.M. Oh, A. Ogata, S. Futamura, Appl. Catal. B: Environ. 56 (2005) 213–220.
[17] F.B. Li, X.Z. Li, Chemosphere 48 (2002) 1103–1111.
[18] J.M. Hermann, A. Sclafani, J. Photochem. Photobiol. A: Chem. 113 (1998) 181–188.
[19] A. Wold, Chem. Mater. 5 (1993) 280–283.
[20] C.Y. Wang, C.Y. Liu, X. Zheng, J. Chen, T. Shen, Colloids Surf. A 131 (1998) 271–280.
[21] J.M. Hermann, J. Disdier, M.N. Mozzanega, P. Pichat, J. Catal. 60 (1979) 369–377.
[22] A. Henglein, J. Phys. Chem. 83 (1979) 2209–2216.
[23] V. Vamathevan, R. Amal, D. Beydoun, G. Low, S. McEvoy, J. Photochem. Photobiol. A: Chem. 148 (2002) 233–245.
[24] D. Duonghong, E. Borgarello, M. Gretzel, J. Am. Chem. Soc. 103 (1981) 4685–4690.
[25] C. He, Y. Xiong, J. Chen, C. Zha, X. Zhu, J. Photochem. Photobiol. A: Chem. 157 (2003) 71–79.
[26] P. Pichat, J. Disdier, J.M. Hermann, P. Vaudano, Nouy. J. Chim. 10 (1986) 545–551.
[27] M.D. Ward, J.R. White, A.J. Bard, J. Am. Chem. Soc. 105 (1983) 27–31.